Impact and modeling of the solar eclipse effects of 20 March 2015 on VLF measurements

Daniela Wenzel, Jens Berdermann, Norbert Jakowski
Institute of Communications and Navigation

E-mail: Daniela.Wenzel@dlr.de

DLR

Outline

1. Global Ionospheric Flare Detection System (GIFDS)
2. Solar eclipse of 20 March 2015
3. Modelling of VLF measurements
4. Final remarks and prospects

Outline

1. **Global Ionospheric Flare Detection System – GIFDS**
2. Solar eclipse of 20 March 2015
3. Modelling of VLF measurements
4. Final remarks and prospects

1. Global Ionospheric Flare Detection System – GIFDS

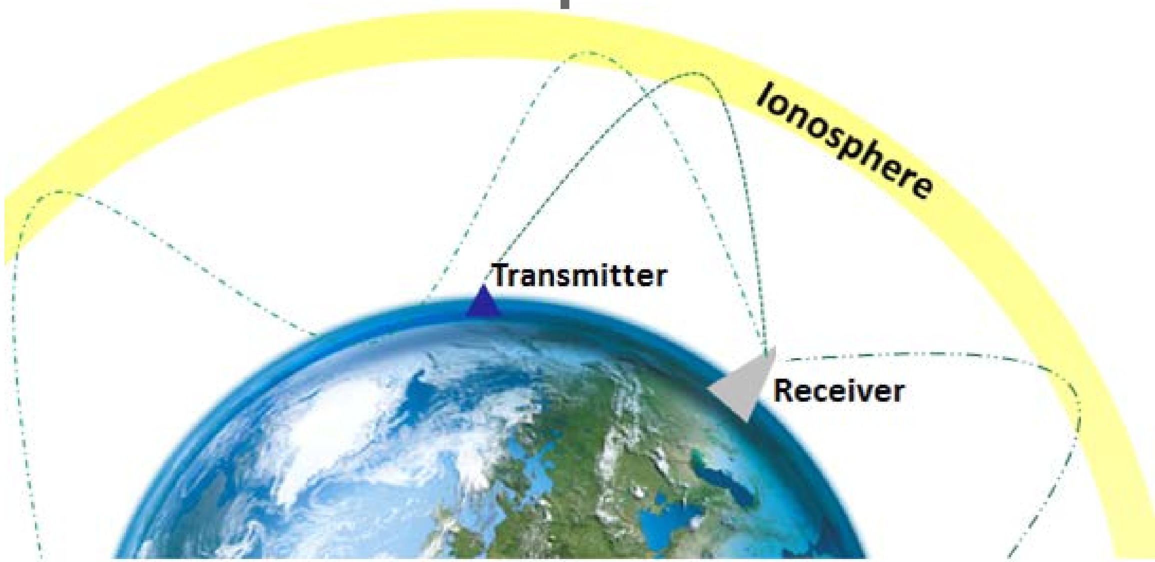

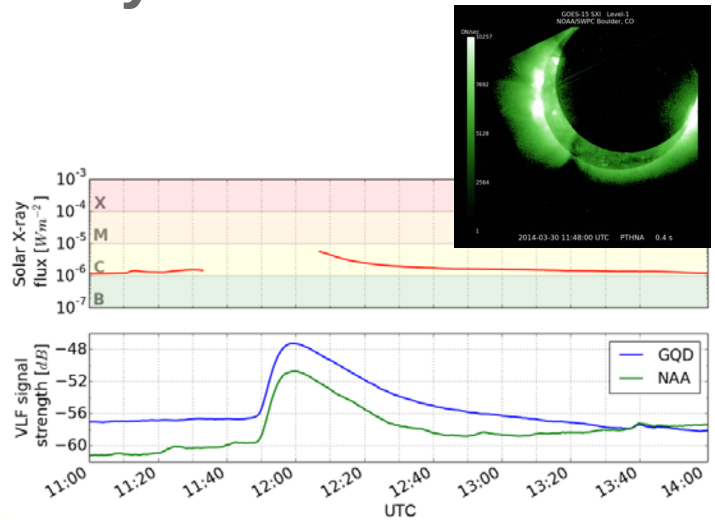

Global Ionospheric Flare Detection System:

- Now cast detection of solar flares using a ground based system
- Measurements of VLF signal strength and phase from 3 to 100 kHz [update rate: 1 Hz]
- Perseus SDR software defined radio and MiniWhip antenna

1. Global Ionospheric Flare Detection System – GIFDS

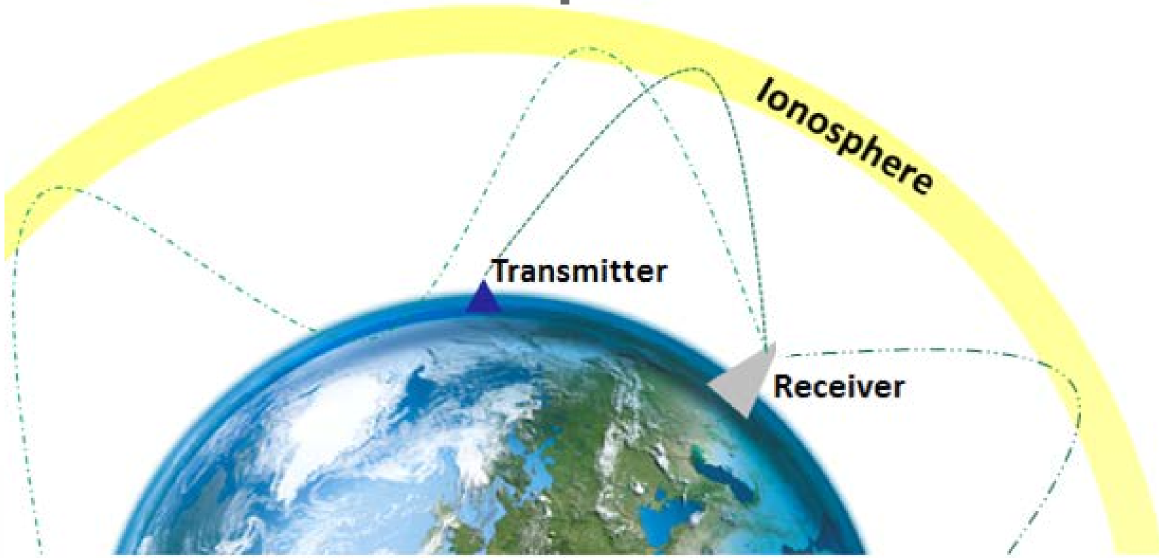

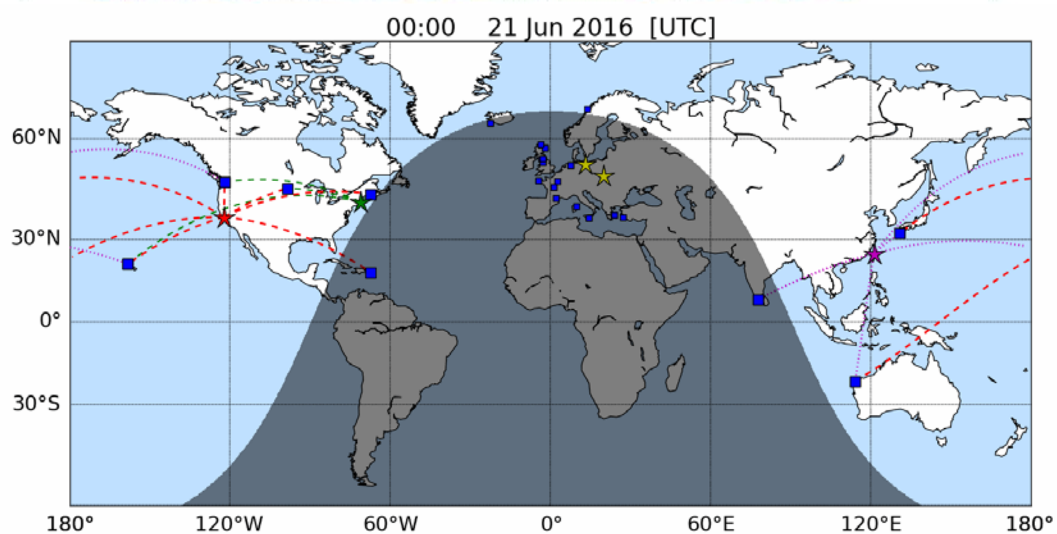

→ **PAPER:** Wenzel et al. 2016

→ **POSTER:**
The German ISWI instruments SOFIE and GIFDS

→ **POSTER:**
German Space Weather Activities

DLR

Outline

1. Global Ionospheric Flare Detection System – GIFDS
2. **Solar eclipse of 20 March 2015**
3. Radio wave propagation
4. Modelling of VLF measurements
5. Final remarks and prospects

2. Total solar eclipse: 20 March 2015

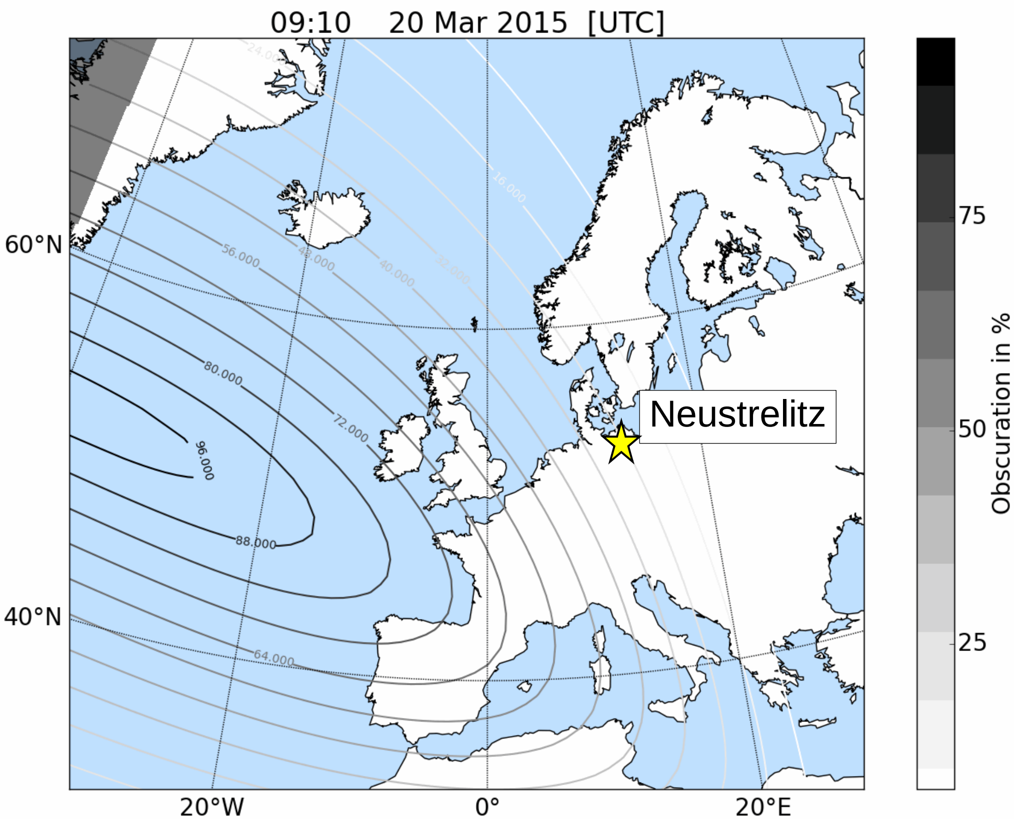

	[UTC]
First contact of penumbra:	07:40
First contact of umbra :	09:09
Greatest Eclipse:	09:46
Last contact of umbra :	10:21
Last contact of penumbra:	11:50

2. Total solar eclipse: VLF measurements

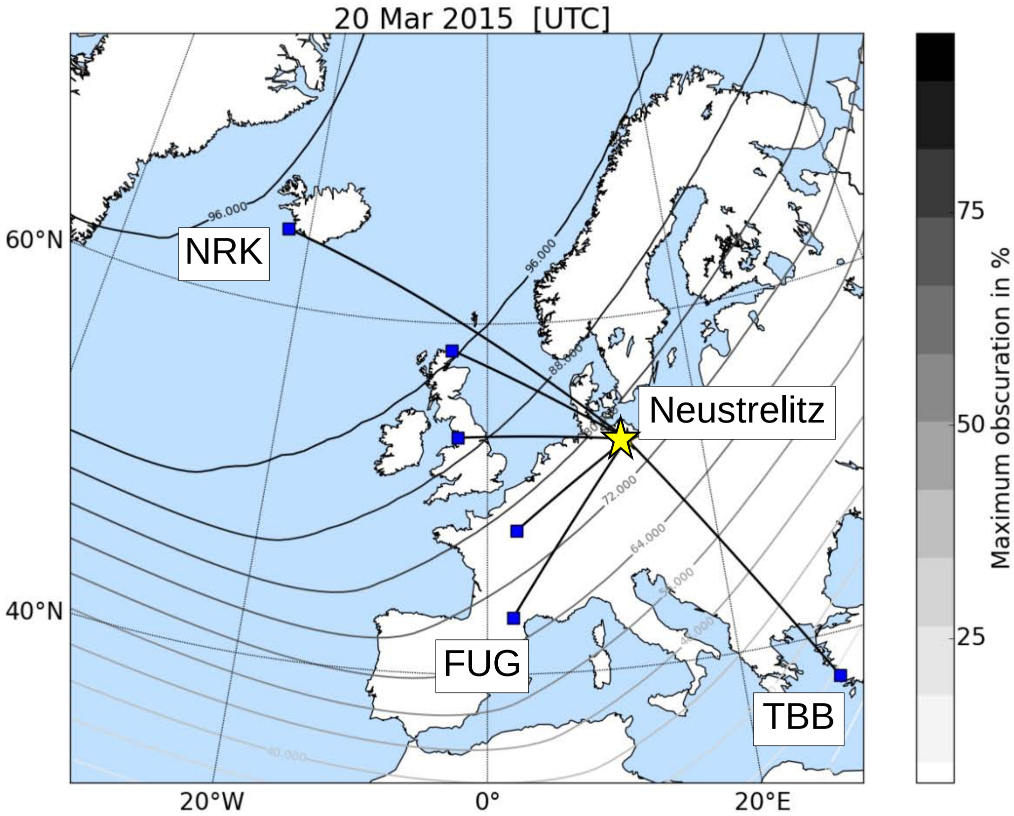

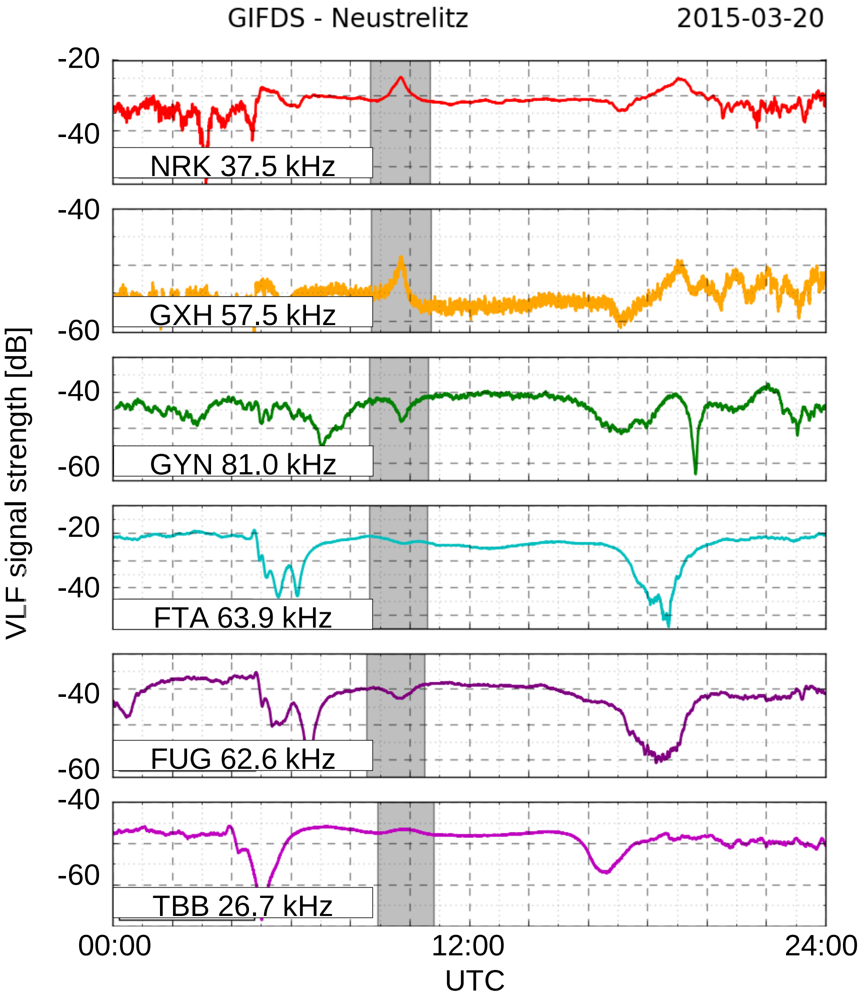

Hoque et al., 2016

2. Total solar eclipse: VLF measurements

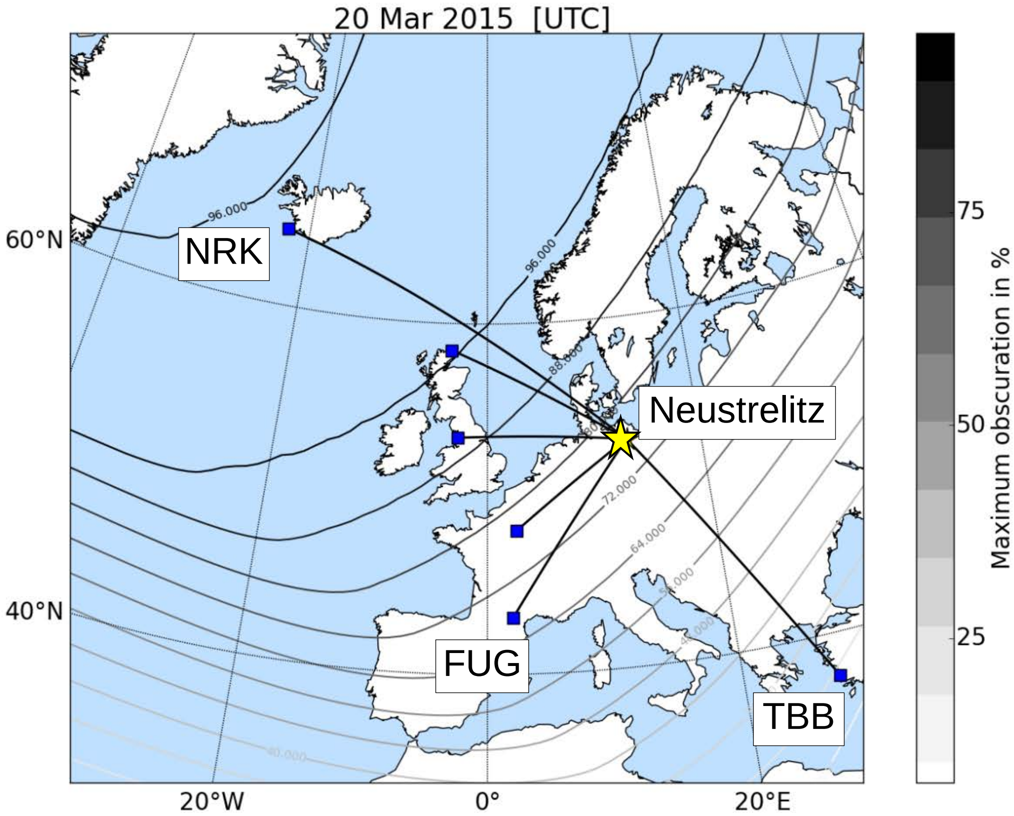

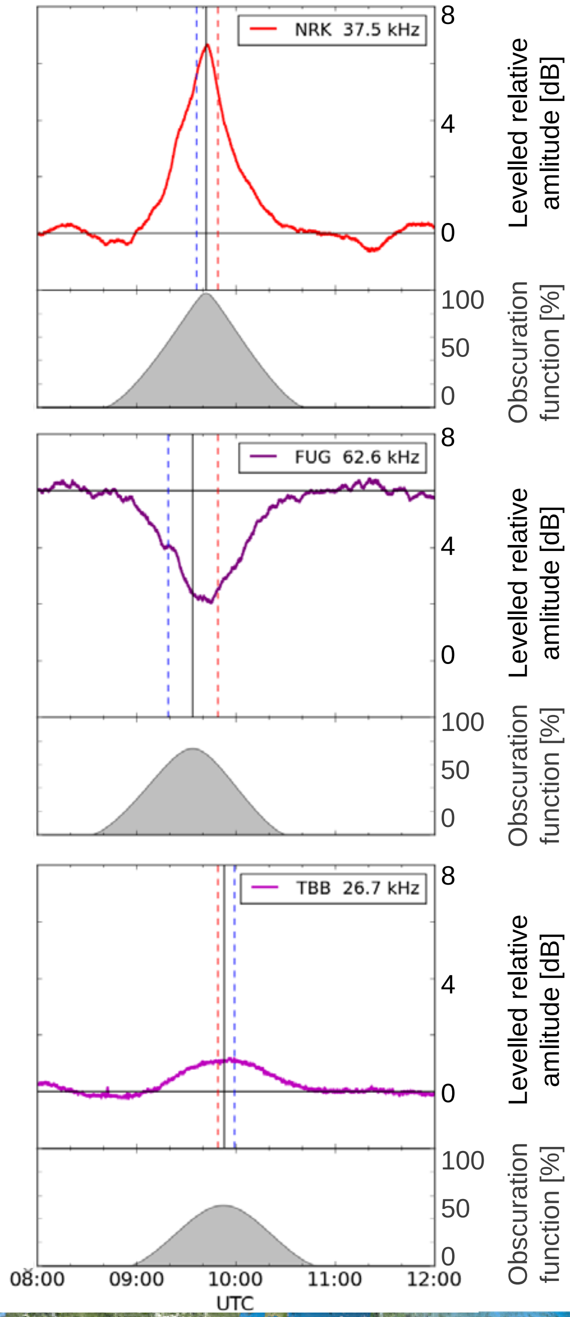

Outline

1. Global Ionospheric Flare Detection System – GIFDS
2. Solar eclipse of 20 March 2015
3. Modelling of VLF measurements
4. Final remarks and prospects

3. Modelling of VLF measurements: LWPC

LWPC – Long-Wavelength Propagation Capability:

- Developed by the Space and Naval Warfare Systems Center, San Diego (Ferguson et al., 1989; 1998)
- Collection of serarate programs written in Fortran and C
- Calculation of field values for VLF propagation in ionospheric waveguide
- Flexibility of input parameters, e.g. ionospheric models

3. Modelling of VLF measurements: LWPC

<u>LWPC – Long-Wavelength Propagation Capability:</u>

- Exponential ionospheric model using h‘ and β (Wait and Spieß, 1964)

$$N_e(h, h', \beta) = 1.43 \times 10^7 \, e^{0.15h'} e^{(\beta - 0.15)(h - h')}$$

- Unperturbed ionosphere model based on latitude, season and time (Thomson, 1993):

$$h' = 74.37 - 8.097 \cos\alpha_{za} + 5.779 \cos\theta - 1.213 \cos\varphi - 0.044\, X_4 - 6.038\, X_5 \; km$$
$$\beta = 0.5349 - 0.1658 \cos\alpha_{za} - 0.08584 \cos\varphi + 0.1296\, X_5 \; km^{-1}$$

$$h' = 76 \; km$$
$$\beta = 0.43 \; km^{-1}$$

3. Modelling of VLF measurements:
VLF measurements

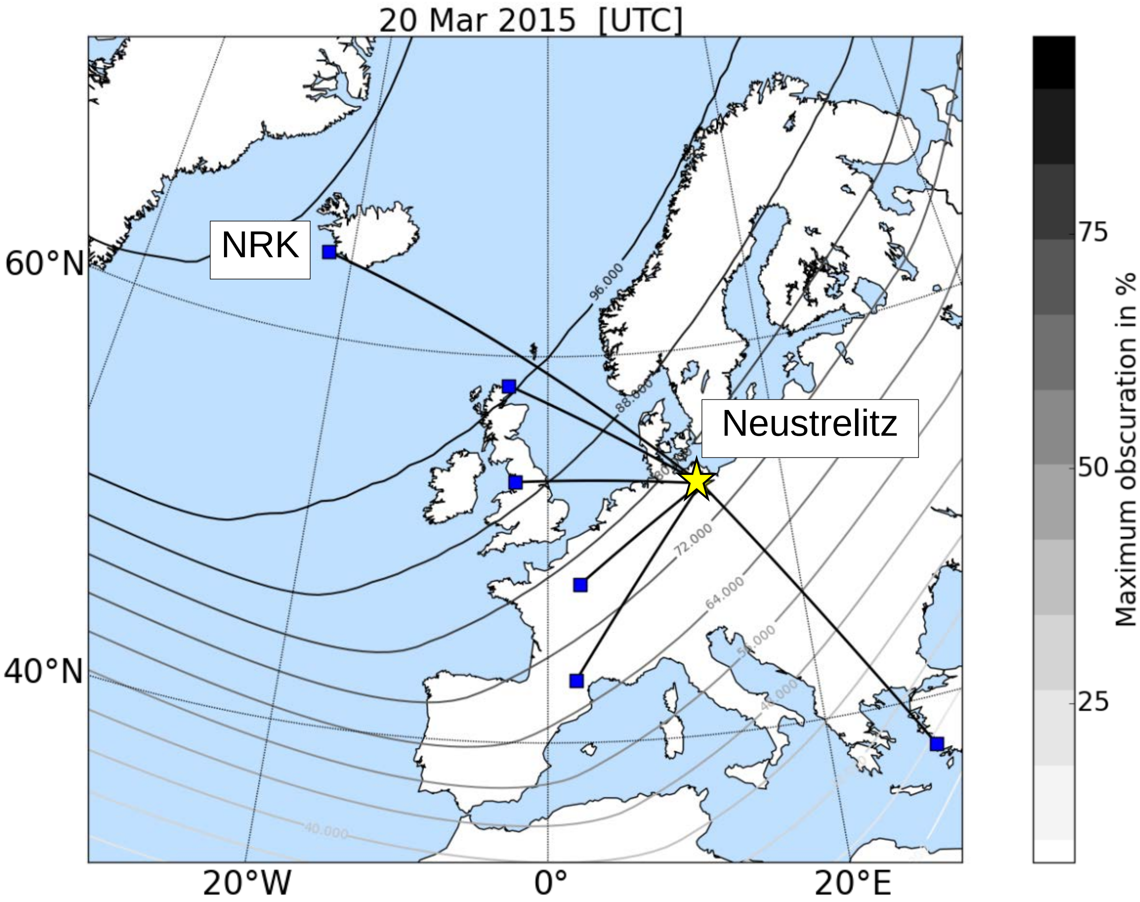

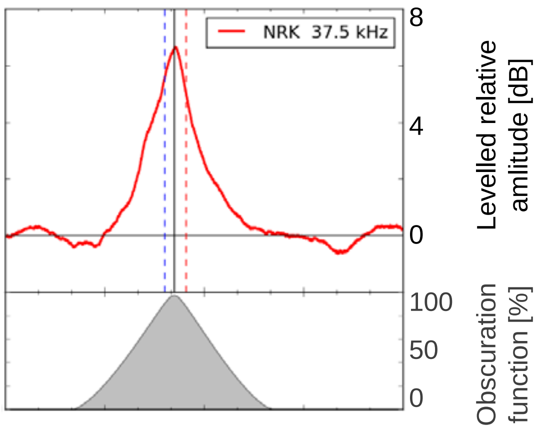

DLR

3. Modelling of VLF measurements:
VLF measurements

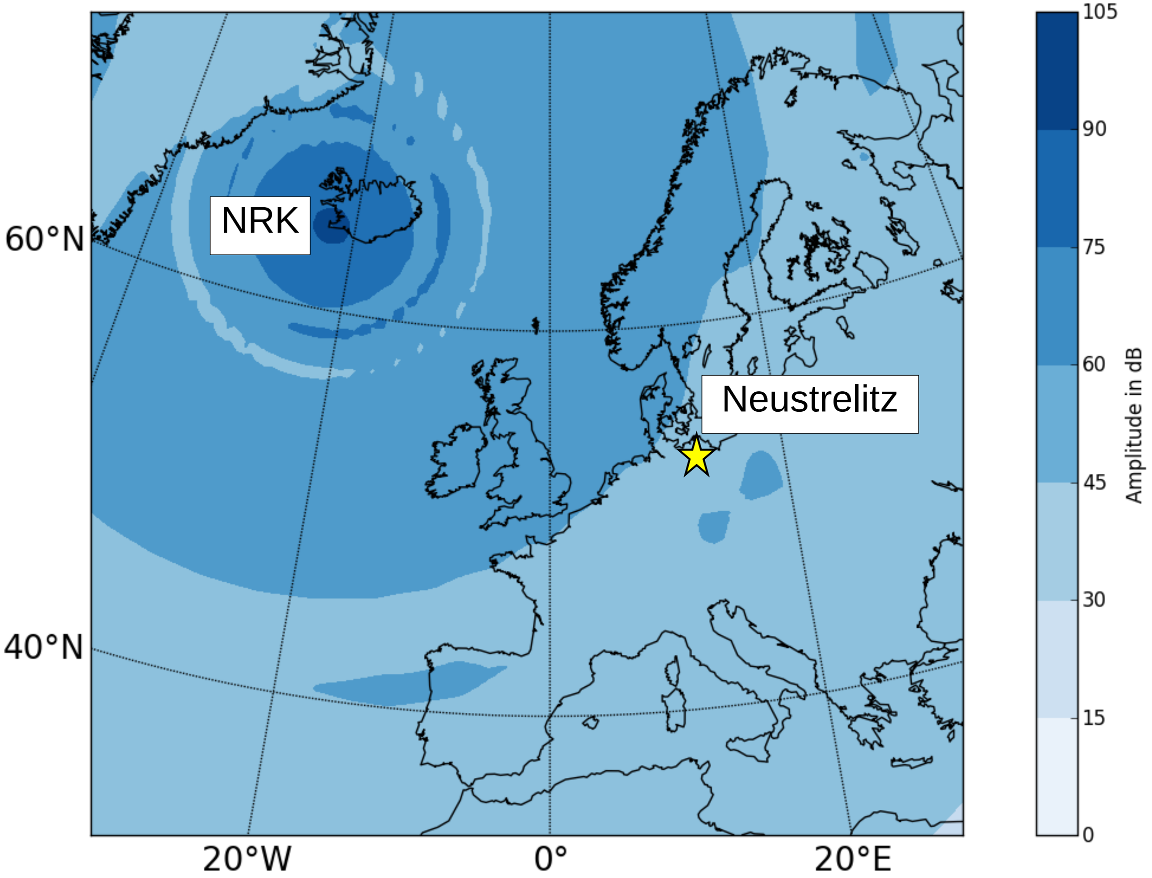

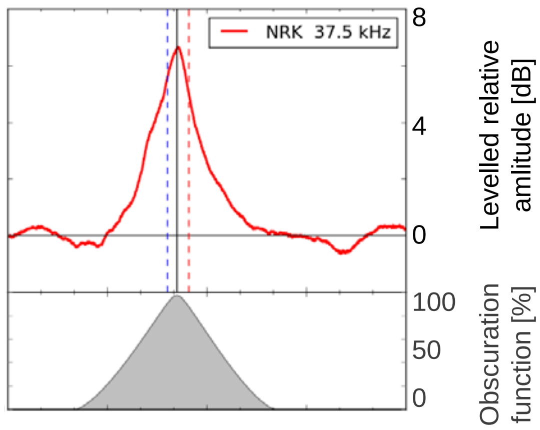

3. Modelling of VLF measurements:
VLF measurements

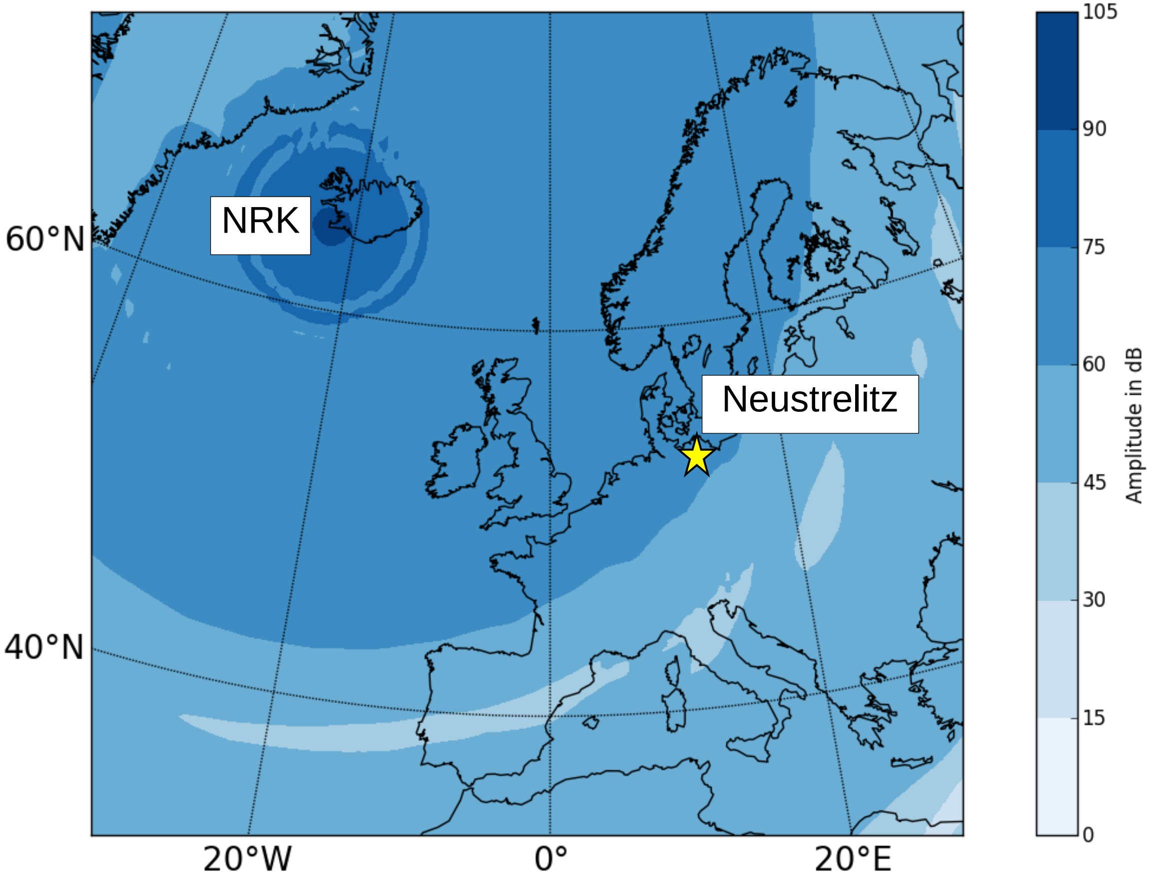

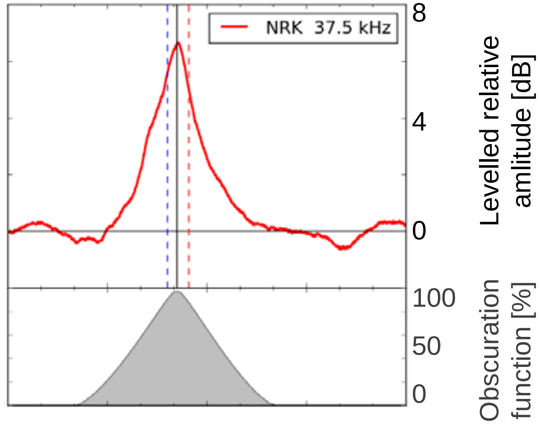

3. Modelling of VLF measurements:
VLF measurements

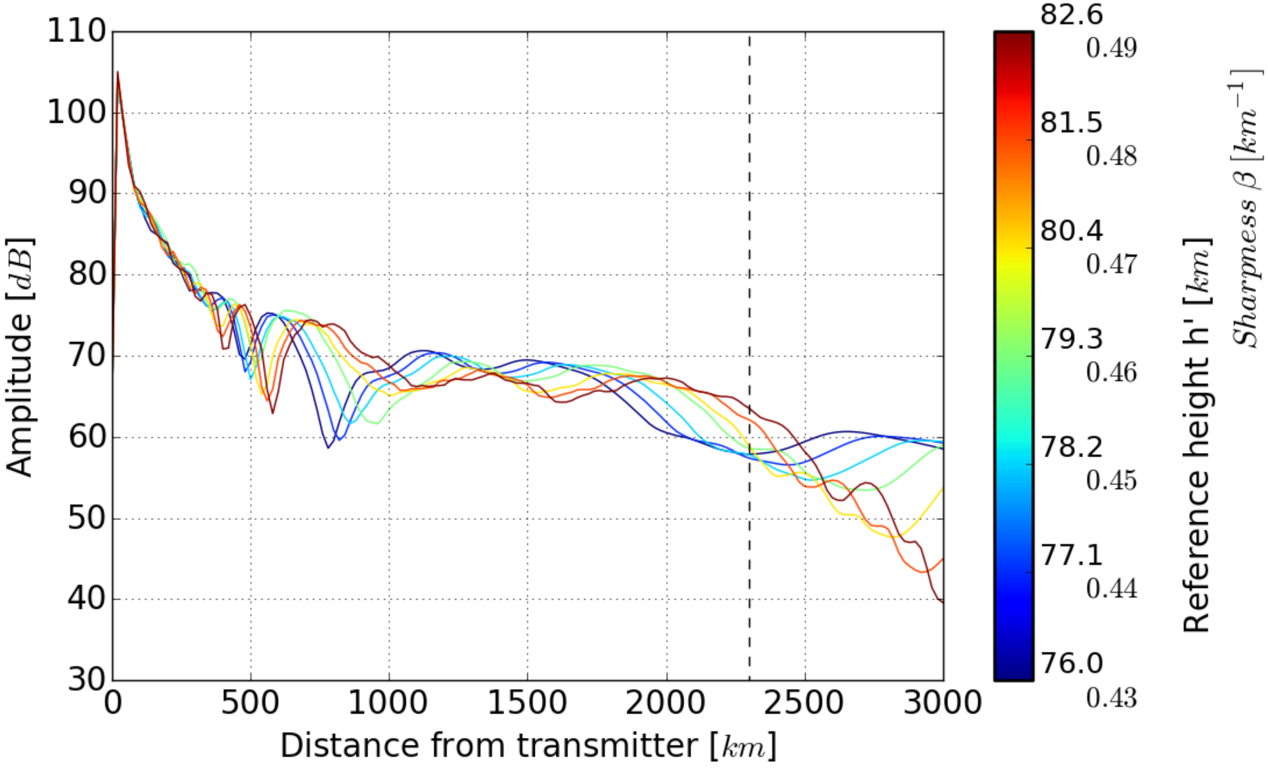

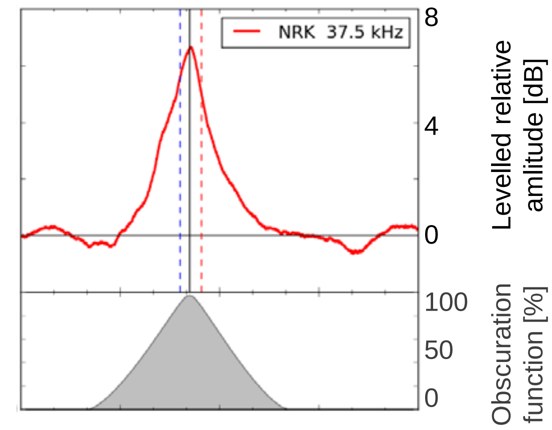

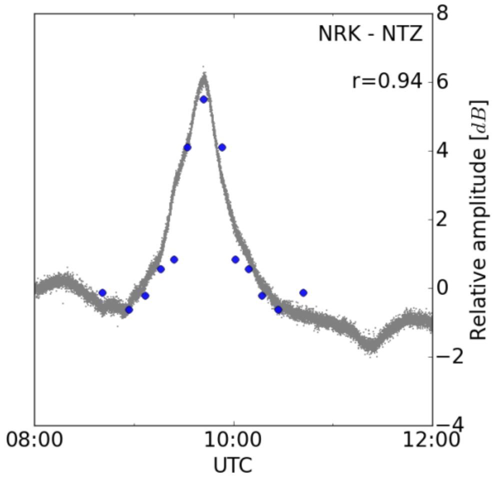

3. Modelling of VLF measurements:
VLF measurements

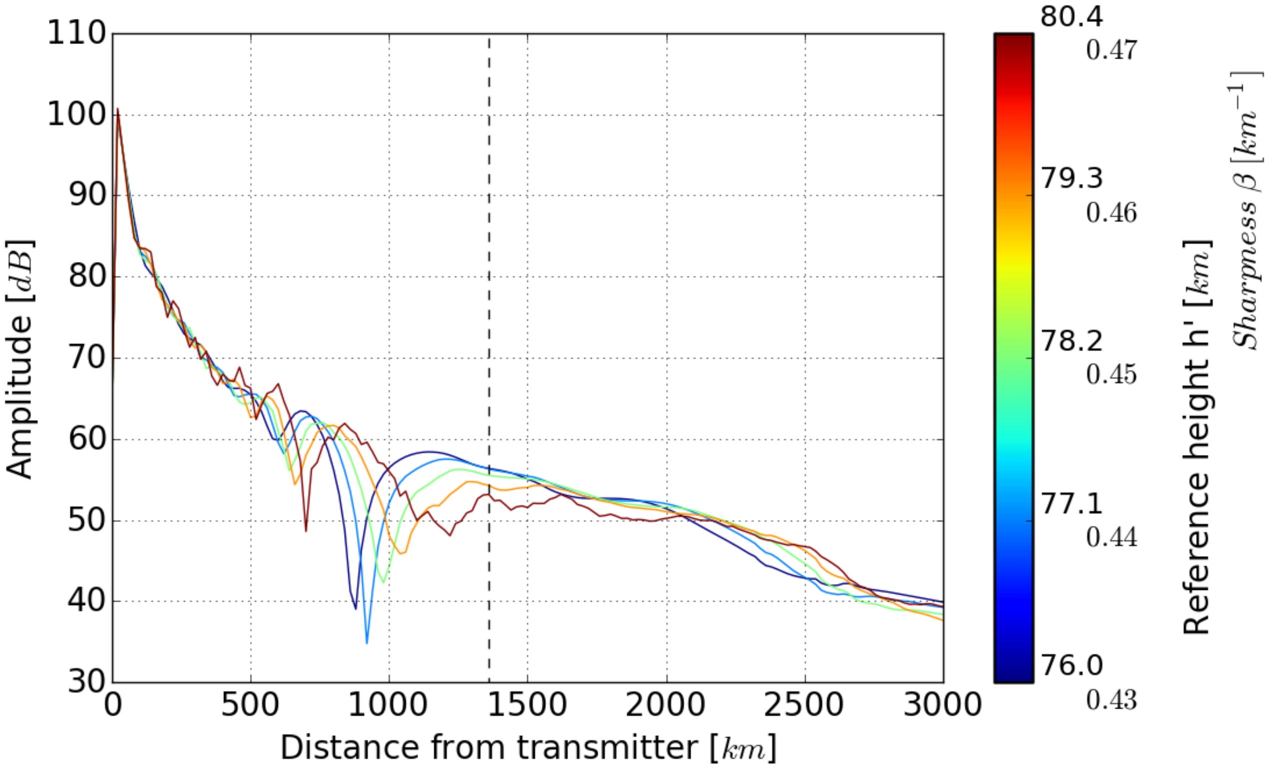

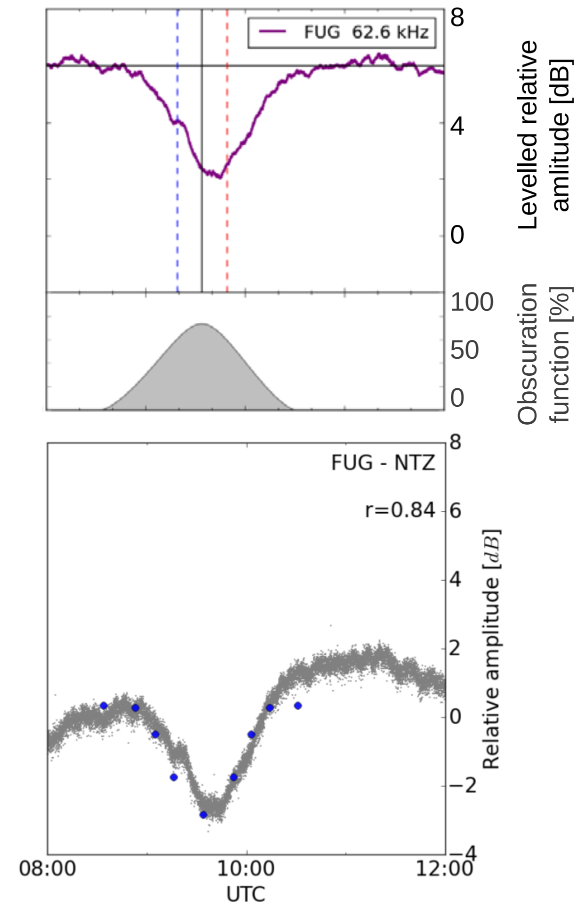

DLR

3. Modelling of VLF measurements:
VLF measurements

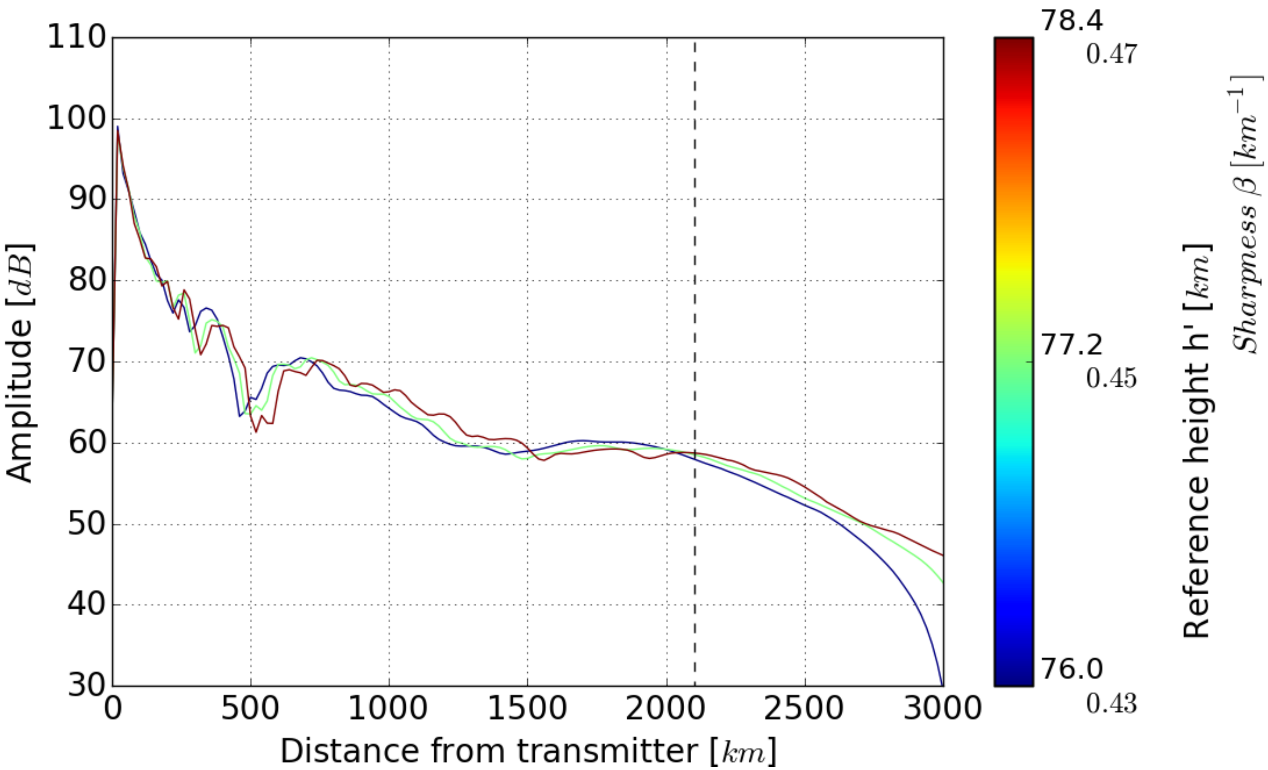

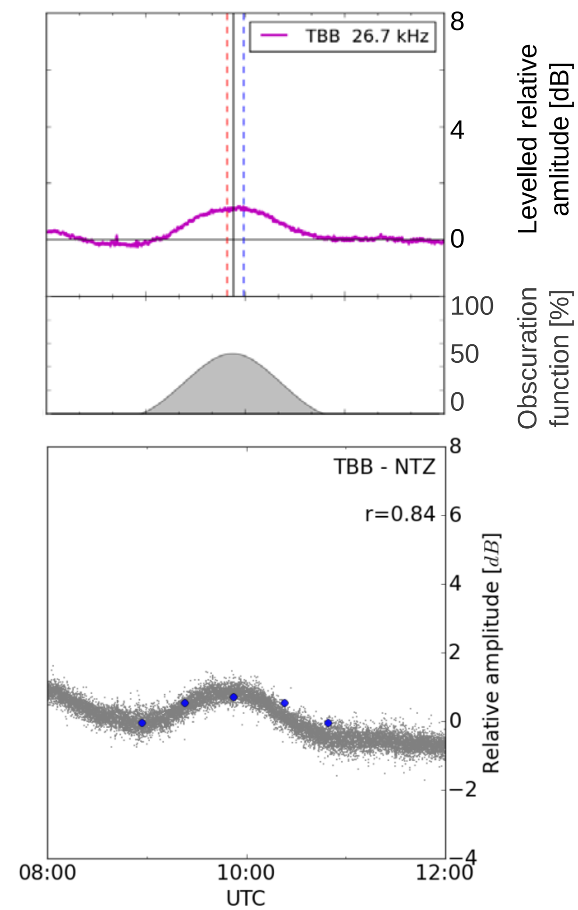

4. Modelling of VLF measurements: Results

NRK: 97% obscuration	FUG: 73% obscuration	TBB: 51% obscuration
$h' = 82.6\ km$ $\beta = 0.49\ km^{-1}$	$h' = 80.4\ km$ $\beta = 0.47\ km^{-1}$	$h' = 78.4\ km$ $\beta = 0.47\ km^{-1}$
$\Delta h' = 6.6\ km$ $\Delta\beta = 0.06\ km^{-1}$	$\Delta h' = 4.4\ km$ $\Delta\beta = 0.04\ km^{-1}$	$\Delta h' = 2.4\ km$ $\Delta\beta = 0.04\ km^{-1}$

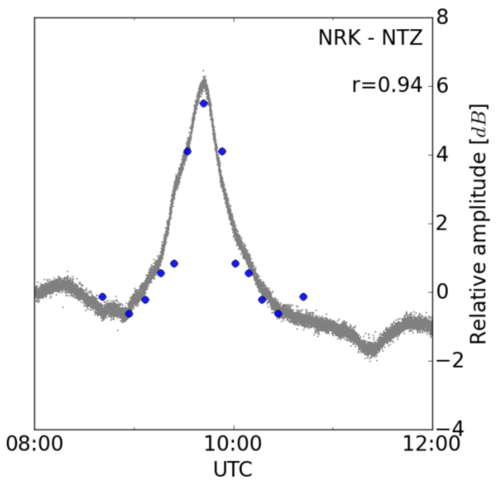

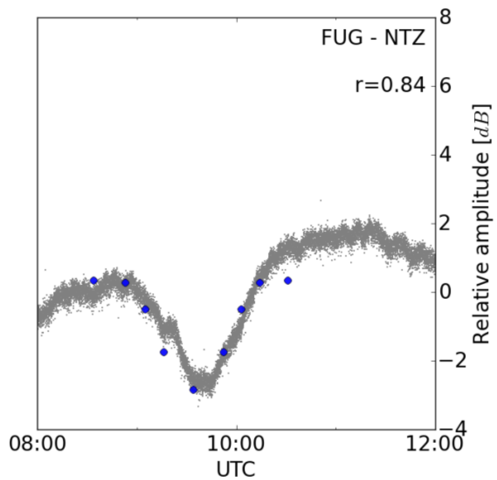

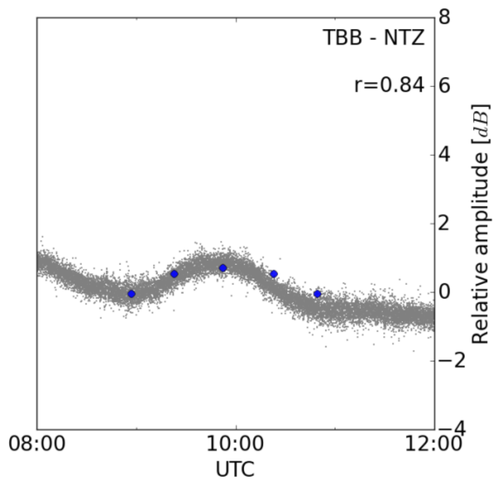

DLR

4. Modelling of VLF measurements: Results

NRK: 97% obscuration

$$h' = 82.6\ km$$
$$\beta = 0.49\ km^{-1}$$

$$\Delta h' = 6.6\ km$$
$$\Delta\beta = 0.06\ km^{-1}$$

FUG: 73% obscuration

$$h' = 80.4\ km$$
$$\beta = 0.47\ km^{-1}$$

$$\Delta h' = 4.4\ km$$
$$\Delta\beta = 0.04\ km^{-1}$$

TBB: 51% obscuration

$$h' = 78.4\ km$$
$$\beta = 0.47\ km^{-1}$$

$$\Delta h' = 2.4\ km$$
$$\Delta\beta = 0.04\ km^{-1}$$

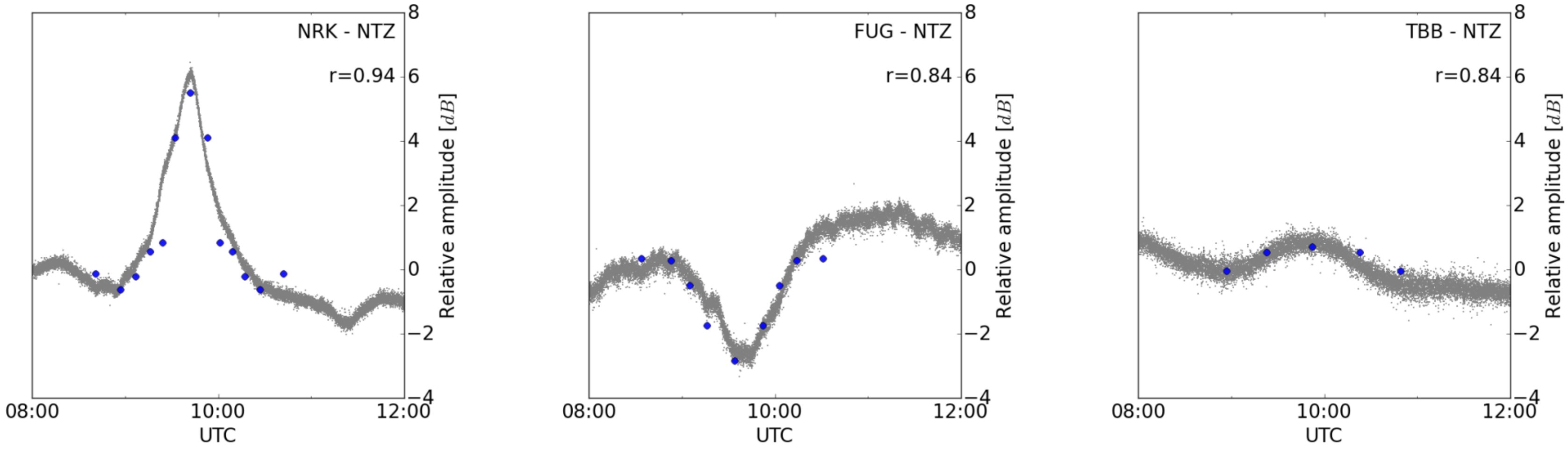

4. Modelling of VLF measurements: Results

NRK: 97% obscuration	FUG: 73% obscuration	TBB: 51% obscuration
$h' = 82.6\ km$	$h' = 80.4\ km$	$h' = 78.4\ km$
$\beta = 0.49\ km^{-1}$	$\beta = 0.47\ km^{-1}$	$\beta = 0.47\ km^{-1}$
$\Delta h' = 6.6\ km$	$\Delta h' = 4.4\ km$	$\Delta h' = 2.4\ km$
$\Delta\beta = 0.06\ km^{-1}$	$\Delta\beta = 0.04\ km^{-1}$	$\Delta\beta = 0.04\ km^{-1}$

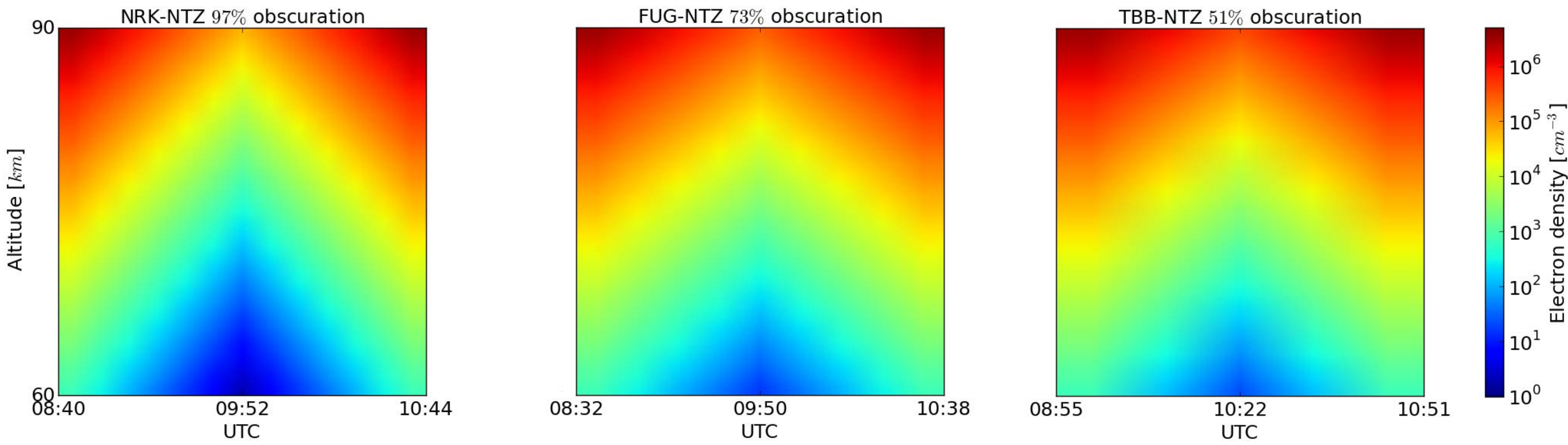

4. Modelling of VLF measurements: Results

NRK: 97% obscuration

$$h' = 82.6\ km$$
$$\beta = 0.49\ km^{-1}$$

$$\Delta h' = 6.6\ km$$
$$\Delta\beta = 0.06\ km^{-1}$$

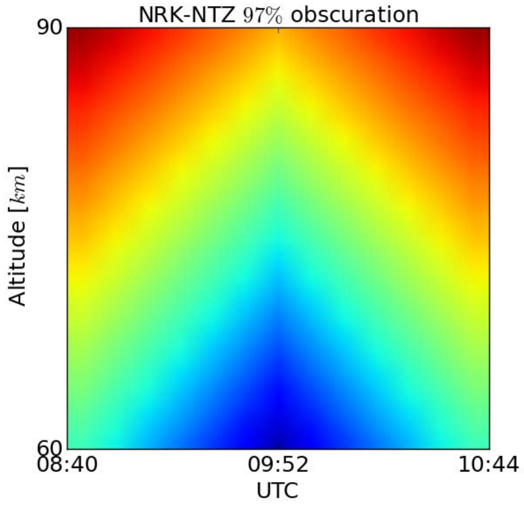

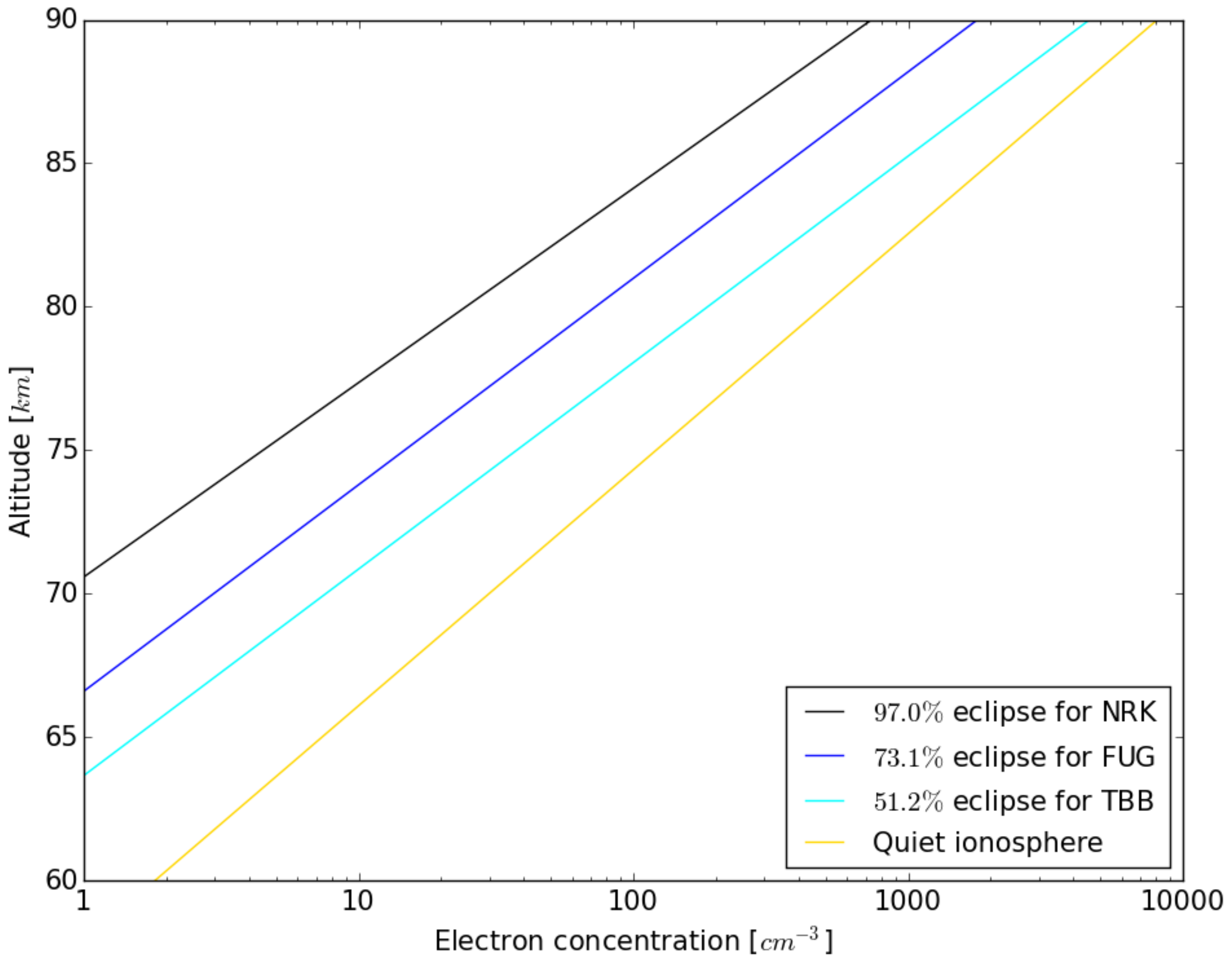

DLR

Outline

1. Global Ionospheric Flare Detection System – GIFDS
2. Solar eclipse of 20 March 2015
3. Modelling of VLF measurements
4. **Final remarks and prospects**

5. Final remarks and prospects:

Summary:

- Amplitude measurements of different VLF transmitters in Neustrelitz
  Frequency range: 25 – 80 kHz
  Short-medium paths: 900 – 2500 km
- Good fit of modelled VLF paths by LWPC with the assumption of a linear change of h‘ and β with obscuration

Future work:

- Modelling of solar eclipse effects of 21 August 2017

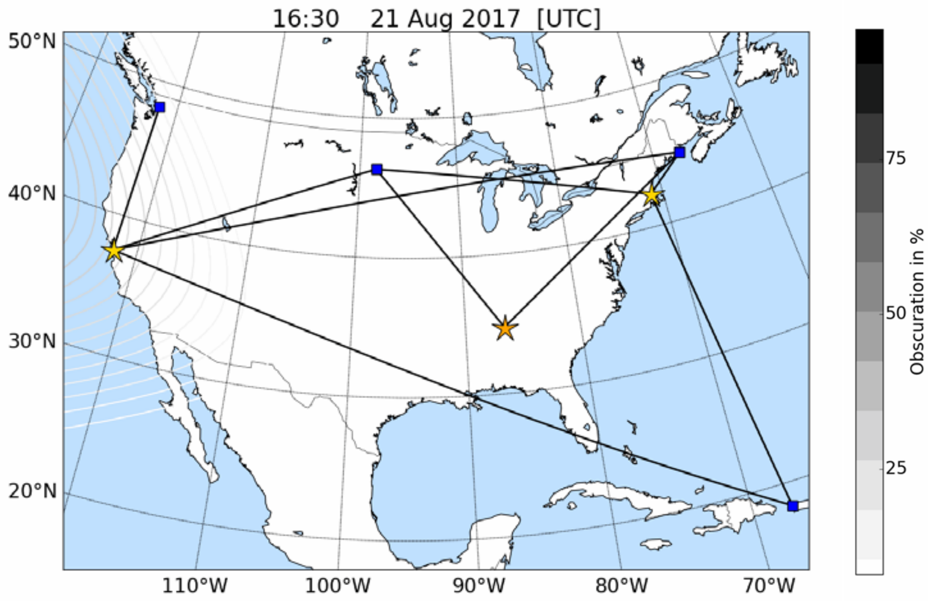

	[UTC]
First contact of penumbra:	15:46
First contact of umbra :	16:48
Greatest Eclipse:	18:25
Last contact of umbra :	20:02
Last contact of penumbra:	21:04

5. Final remarks and prospects:

Summary:

- Amplitude measurements of different VLF transmitters in Neustrelitz
  Frequency range: 25 – 80 kHz
  Short-medium paths: 900 – 2500 km
- Good fit of modelled VLF paths by LWPC with the assumption of a linear change of h‘ and β with obscuration

Future work:

- Modelling of solar eclipse effects of 21 August 2017

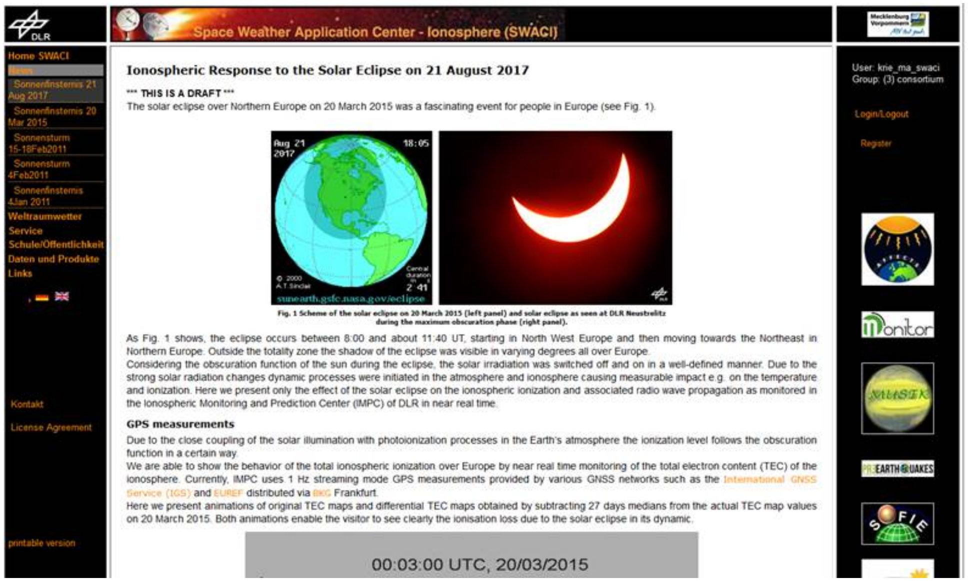
Space Weather Application Center - Ionosphere (SWACI)

Ionospheric Response to the Solar Eclipse on 21 August 2017

*** THIS IS A DRAFT ***

The solar eclipse over Northern Europe on 20 March 2015 was a fascinating event for people in Europe (see Fig. 1).

Fig. 1 Scheme of the solar eclipse on 20 March 2015 (left panel) and solar eclipse as seen at DLR Neustrelitz during the maximum obscuration phase (right panel).

As Fig. 1 shows, the eclipse occurs between 8:00 and about 11:40 UT, starting in North West Europe and then moving towards the Northeast in Northern Europe. Outside the totality zone the shadow of the eclipse was visible in varying degrees all over Europe.

Considering the obscuration function of the sun during the eclipse, the solar irradiation was switched off and on in a well-defined manner. Due to the strong solar radiation changes dynamic processes were initiated in the atmosphere and ionosphere causing measurable impact e.g. on the temperature and ionization. Here we present only the effect of the solar eclipse on the ionospheric ionization and associated radio wave propagation as monitored in the Ionospheric Monitoring and Prediction Center (IMPC) of DLR in near real time.

GPS measurements

Due to the close coupling of the solar illumination with photoionization processes in the Earth's atmosphere the ionization level follows the obscuration function in a certain way.

We are able to show the behavior of the total ionospheric ionization over Europe by near real time monitoring of the total electron content (TEC) of the ionosphere. Currently, IMPC uses 1 Hz streaming mode GPS measurements provided by various GNSS networks such as the International GNSS Service (IGS) and EUREF distributed via BKG Frankfurt.

Here we present animations of original TEC maps and differential TEC maps obtained by subtracting 27 days medians from the actual TEC map values on 20 March 2015. Both animations enable the visitor to see clearly the ionisation loss due to the solar eclipse in its dynamic.

00:03:00 UTC, 20/03/2015

→LIVE web broadcast of ionospheric observation including VLF, NRT TEC minus median TEC , slab thickness, etc.

http://swaciweb.dlr.de/news/sonnenfinsternis-21-aug-2017/?L=0

Thank you for your attention